Polym. Bull. (2010) 65:425–442
DOI 10.1007/s00289-009-0218-9

ORIGINAL PAPER

Novel hyperbranched poly (amine-ester)-poly (lactide-co-glycolide) polymeric micelles as amphotericin B carriers

Tiewei Wang · Yan Wu · Mingjun Li

Received: 31 May 2009 / Revised: 5 November 2009 / Accepted: 21 November 2009 /
Published online: 28 November 2009

Abstract A series of amphiphilic hyperbranched poly (amine-ester)-poly (lactide-co-glycolide) (HPAE-co-PLGA) copolymers were synthesized by ring-opening polymerization of DL-lactide, glycolide and a fourth generation hyperbranched poly (amine-ester) (HPAE-OHs4) with $Sn(Oct)_2$ as catalyst. The chemical structure of copolymers was characterized by Fourier transform infrared (FT-IR), nuclear magnetic resonance (^{1}H-NMR, ^{13}C-NMR), thermo gravimetric analysis apparatus (TGA), and different scanning calorimetry (DSC). Formation and characteristics of polymeric micelles of the amphiphilic copolymer were studied by environmental scanning electron microscopy (ESEM), fluorescence spectroscopy, and dynamic light scattering (DLS). In order to estimate the feasibility as novel drug carriers, a lipophilic model drug amphotericin B was incorporated into polymeric micelles and the drug release behavior was investigated. The micelle size and drug-loading content were found increased, and the drug-release rate decreased with the increase of molar ratio of DL-lactide/glycolide to HPAE.

Keywords Hyperbranched poly (amine-ester) · Poly (lactide-co-glycolide) · Polymeric micelles · Amphotericin B · Drug delivery

T. Wang · Y. Wu (✉)
National Center for Nanoscience and Technology, No. 11 Beiyitiao, Zhongguancun, Beijing 100190, China
e-mail: wuyan66@eyou.com

T. Wang
China Agricultural University, Beijing 100083, China

M. Li
The first affiliated Hospital of Jiamusi University, Jiamusi 154002, China

Introduction

Polymeric micelles consisting of hydrophilic and hydrophobic segments have received special attention due to their potential application and academic interest in many interdisciplinary fields [1–5]. These core–shell type micelles may be used as drug delivery vehicles for poorly water-soluble drugs. The most widely studied amphiphilic polymers for drug delivery are diblock and triblock copolymers. However, these conventional micelle drug delivery systems are based on the linear amphiphilic copolymers with insufficient reactive groups at molecular chains, low encapsulation efficiency, which limit further modification, ligand coupling, and their application in drug delivery [6–11]. In contrast, dendrimers and hyperbranched polymers, with good hydrophilicity and biocompatibility, seem to be attractive alternatives to PEG hydrophilic segments for designing amphiphilic graft copolymers. Since the molecular branching of amphiphilic copolymers is the most important factor in determining micellar structure and property, research efforts have thus focused on the design of molecular structures of amphiphilic copolymers. Recently, amphiphilic copolymers with nonlinear structure exhibited improved property as drug carriers in many researches [12]. Polymeric micelles compositing of branched copolymers may have special application for drug delivery due to their abundant terminal groups.

Over the past two decades, hyperbranched polymers have received extensive research attention as a new class of polymers with unique chain structure. Distinct from their linear analogs, hyperbranched polymers have structures and topologies similar to those of dendrimers, having strikingly superior material properties, such as low solution/melt viscosity, enhanced solubility, abundant terminal groups, etc. [13, 14]. Furthermore, unlike dendrimers that often require tedious synthetic procedures [15], hyperbranched polymers are more easily produced in a large scale, which encourages their potential use in a variety of important applications, including rheological additives, toughening agents, drug delivery etc. [16–20]. Hyperbranched polymers contain numerous end groups in their molecular structures and the characteristics of these terminal groups have a great influence on the properties of resulting hyperbranched polymers. Therefore, modification of number and type of end groups can be a powerful tool to tailor the properties of hyperbranched polymers [21–23].

Recent trends in drug delivery technology have focused on biodegradable polymers requiring no surgical removal once the drug supply is depleted. PLGA is a well-known biodegradable and biocompatible material with a hydrophobic character. In addition, it was reported that DL-lactide and glycolide with other material such as PEG degraded much more rapidly than PLGA homopolymer. The lactide/glycolide polymers chains can be cleaved by hydrolysis into natural metabolites (lactic and glycolic acid), which are eliminated from the body by the citric acid cycle. It is for this reason that PLAG has been extensively used for controlled drug delivery systems. PLGA provides a wide range of degradation rates, from months to years, depending on its composition and molecular weight. Compared to PLA, PLGA improves the crystallinity, permeability, hydrophilicity of PLA homopolymer and enables adjustment to the degradation rate and mechanic intensity of PLA

itself. It can also be used to control drug-release rate by adjustment to the ratio of lactide/glycolide, which facilitates the application for drug delivery.

The present work is to associate the merits of HPAE-OHs and PLGA and prepared HPAE-co-PLGA polymeric micelles as drug carriers. If PLGA can be grafted onto hydroxyl groups of HPAE-OHs, the amphiphilic copolymers would become affordable. Owing to the introduction of hydrophilic HPAE-OHs molecules, a drug can be encapsulated into the HPAE-co-PLGA polymeric micelles without any deactivation. The new hyperbranched polymeric micelles contained abundant terminal groups, which enable binding drug with other target groups for drug delivery system. For this purpose, we synthesize the HPAE-co-PLGA copolymers by opening polymerization with hyperbranched HPAE, DL-lactide, and glycolide. The chemical structure and physical properties of copolymers were characterized and the formation of polymeric micelle was investigated. Finally, the lipophilic drug amphotericin B, first-line treatment for intraocular fungal infections [24, 25], was incorporated into polymeric micelles as a model drug and the drug release behavior was investigated.

Experimental

Materials

1,1,1-Trimethylol propane of reagent grade, methyl acrylate (purified by vacuum distillation), and diethanolamine were purchased from National Medicines Chemical Reagent Co. Ltd (China.). Titanium tetraisopropoxide ($Ti(OiPr)_4$, benzoic anhydride, and imidazole were purchased from Beijing Reagent Factory,(China). DL-Lactide and glycolide were purchased from PURAC (The Netherlands) and used without further purification. $Sn(Oct)_2$ was purchased from Sigma (America). Amphotericin B was purchased from Shanghai Xinxianfeng Pharmaceutical Co. (Shanghai, China). All other reagents were analytical grade.

Synthesis and characterization of HPAE-co-PLGA copolymer

HPAE-OHs were synthesized through a pseudo-one-step process by alcoholysis. The second-generation HPAE-OHs4 was obtained as follows: first, 1,1,1-trimethylol propane (as a molecular core) reacted with *N*, *N*-diethylol-3-amine methylpropionate (as an AB_2 monomer) in N_2 at 120 °C for 12 h with $Ti(OiPr)_4$ (1%, w/w) as the catalyst. The feed molar ratio of 1,1,1-trimethylol propane to *N*, *N*-diethylol-3-amine methylpropionate was 1:9. Then the obtained product was dissolved in 10 mL ethanol with $Ti(OiPr)_4$ precipitated and the $Ti(OiPr)_4$ was removed by filtration. Finally, ethanol was evaporated and the product was dried at 40 °C in a vacuum oven and stored for further utilization.

The generation of HPAE-OHs was increased by repeatedly adding *N*, *N*-diethylol-3-amine methylpropionate monomer to the former generation product.

N, *N*-diethylol-3-amine methylpropionate was prepared by using methyl acrylate and diethanolamine in methanol under N_2 at 35 °C for 5 h. The feed molar ratio of

methyl acrylate to diethanolamine is 1.5:1. After the Michael reaction, excess methyl acrylate and methanol were removed through vacuum distillation.

The fourth generation HPAE-OHs4 was obtained by repeating the process three times.

HPAE-co-PLGA copolymer was synthesized through a ring-opening polymerization procedure. DL-Lactide (DLLA), glycolide, and HPAE-OHs4 were dehydrated by using P_2O_5 under vacuum at 45 °C for 24 h and used without further purification. A total of 50 g of DL-lactide, glycolide plus HPAE-OHs4 were used for the polymerization. Copolymerization in the bulk state was carried out with various molar ratios of DL-lactide/glycolide (6/1, 10/1, and 15/1) and the weight ratio of HPAE-OHs4 was adjusted to 30% (w/w). $Sn(Oct)_2$ (0.2%, w/w) was added into a dried polymerization tube followed by the addition of DL-lactide, glycolide, and HPAE-OHs4. The polymerization tube was sealed under vacuum and kept in an oil bath at 150 °C. After 13 h, the product was cooled to ambient temperature. The obtained viscous material was dissolved with CH_2Cl_2 and then precipitated with ether/petroleum (1:1, v/v) to remove unreacted DL-lactide, glycolide monomers. After ether and the petroleum were evaporated, the copolymers were dissolved in a little of acetone and then precipitated in deionized water. The purified copolymers were dried at 40 °C for 2 days in a vacuum oven.

Characterization of HPAE-OHs and HPAE-co-PLGA copolymer

The FT-IR spectra of HPAE-OHs was recorded on Fourier transform infrared (FT-IR) spectrometer (Spectrum One Perkin-Elmer, America) using a film as reference. The HPAE-co-PLGA samples were mixed with KBr and pressed to a plate for measurement.

The nuclear magnetic resonance (^{1}H-NMR, ^{13}C-NMR) of HPAE-OHs and HPAE-co-PLGA copolymer was recorded on a (Bruker AVANCE 400) NMR spectrometer. HPAE-OHs were dissolved in DMSO-*d*6 and HPAE-co-PLGA copolymers were dissolved in $CDCl_3$.

Gel permeation chromatography (GPC) was performed on a Waters 2410 GPC apparatus (USA). Molecular weight and molecular weight distribution of the copolymers were calculated using polystyrene as the standard.

The thermal stability of HPAE-OHs4 and HPAE-co-PLGA samples was measured using TGA (Perkin-Elmer, America). The temperature range was carried out from 25 to 900 °C under nitrogen flow with heating rate of 20 °C/min.

The thermo-property of HPAE-OHs4, PLGA, and HPAE-co-PLGA samples was also measured using DSC. Samples (3–5 mg) were loaded into aluminum pans and the DSC thermo grams were recorded on a Pyris Diamond DSC apparatus (Perkin-Elmer, America). In order to observe T_g, all of the DSC thermo grams were obtained with a second heating procedure. Briefly, the heating rate was 20 °C/min in the range of 20–100 °C by using nitrogen flowing, samples were stored at 100 °C for 1 min and then cooled to −50 °C, the cooling rate was 20 °C/min, then the samples were re-heated from 0 to 100 °C in the heating rate of 20 °C/min.

Determination of the hydroxyl values of HPAE-OHs

The hydroxyl values of HPAE-OHs were determined as described in the previous paper [26]. HPAE-OHs were dissolved in excess benzoic anhydride with imidazole as a catalyst at 80 °C for 3 h. The benzoic anhydride was used to acetylate the hydroxyl groups in HPAE-OHs. By back-titrating the above mixture with NaOH solution (0.1 mol L^{-1} in water) at room temperature, the hydroxyl values of HPAE-OHs were calculated.

Preparation of amphotericin B-loaded HPAE-co-PLGA polymeric micelle

The HPAE-co-PLGA polymeric micelle was prepared according to the previous paper [27] with slight modification. Amphotericin B and HPAE-co-PLGA copolymer were dissolved in 5 mL of DMSO. This solution was slowly dripped into 20 mL deionized water (or 0.25%, w/v, Pluronic F-68) for 10 min and then stirred for another 5 min to form polymeric micelle. Then the solution was introduced into a dialysis tube (MWCO 8,000 g/mol) and dialyzed against deionized water (or with 0.25% Pluronic F-68) for 24 h to remove the solvent. The dialyzed solution was filtered through 1.0 μm syringe filter and then lyophilized or analyzed.

Plain polymeric micelles of HPAE-co-PLGA copolymers were prepared by the same procedure as described above with the exception of amphotericin B.

Characterization of the HPAE-co-PLGA polymeric micelles

Environmental scanning electron microscopy (ESEM, Quauta 200FEG, FEI) was used to observe the morphology of the micelles. A drop of micelle solution was deposited onto a silicon chip and air-dried before ESEM observation.

The size and size distribution of polymeric micelles were measured using a DLS (Zetasizer Nano series ZEN 3600Malvern Instruments Ltd., England) with a wavelength of 532 nm and detection angle of 90° at 25 °C.

Steady-state fluorescence spectrum was recorded on a spectrofluorophotometer (FL-920 England). The solution of HPAE-co-PLGA copolymers containing 6×10^{-7} M of pyrene was placed in a square cell and the fluorescence spectrum was obtained with a fluorophotometer. The concentration of the sample solution varied from 1.0×10^{-3} to 0.5 mg/mL and the excitation wavelength (λ_{ex}) was 336 nm.

Biodegradation of the HPAE-co-PLGA copolymer and HPAE-co-PLGA copolymer micelle

20 mg samples of the HPAE-co-PLGA copolymers and their micelle lyophilized powder were compressed with a mold into a film on a Carver Laboratory Press (Fred S. Carver Inc., USA) at room temperature.

$$\text{Biodegradation}\,(\%) = 100(W_1 - W_d)/W_1,$$

where W_1 and W_d represents the dried weight of the original film and the weight after incubating in PBS (pH 7.4) at 37 °C for specific days, respectively.

Micelle yield, drug-loading content, and entrapment efficiency

The resulted micellar solution was frozen and lyophilized to obtain the dried product. In order to evaluate the drug contents and loading efficiency, 5 mg of amphotericin B-loaded HPAE-co-PLGA polymeric micelle was dissolved in 10 mL of DMSO and then diluted with DMSO. The concentration of amphotericin B was evaluated using an UV-spectrophotometer (Perkin Elmer Lambda850 [USA]) at 415 nm. Empty polymeric micelle of HPAE-co-PLGA copolymer was used as a blank test. The micelle yield, drug-loading content, and drug entrapment efficiency were presented by Eqs. 1–3, respectively

$$\text{Micelle yield}\,(\%) = \text{weight of micelles/weight of polymer and drug feed initially} \times 100 \quad (1)$$

$$\text{Drug-loading content}\,(\%) = \text{weight of drug in micelles/weight of micelles} \times 100 \quad (2)$$

$$\text{Entrapment efficiency}\,(\%) = \text{weight of drug in micelles/weight of drug feed initially} \times 100 \quad (3)$$

Each sample was assayed in triplicate.

Physical stability of amphotericin B-loaded polymeric micelles

The drug-loaded micelles were determined for physical stability in PBS. Micellar diameter changes were evaluated by DLS as mentioned above.

In vitro release

During in vitro release experiment, 5 mg of lyophilized amphotericin B-loaded HPAE-co-PLGA polymeric micelles was reconstituted into 5 mL of PBS and then introduced into dialysis tube (MWCO 12,000 g/mol). The dialysis tubes were placed in 200 mL bottle with 95 mL of PBS, and the media stirred at 37 °C and 100 ppm using a magnetic stirrer. The media was taken out for drug concentration analysis at specific time intervals. After that, whole media was replaced with fresh PBS to prevent drug saturation. Then the media was diluted 10–100 times with DMSO and the concentration of the amphotericin B released was determined using an UV-spectrophotometer (Perkin Elmer Lambda850 [USA]) at 415 nm. Since the properties of UV spectrum of amphotericin B in DMSO do not change in the range between 0.1 and 10 μg/mL, we diluted the release medium with DMSO to this range for drug concentration estimation using UV-spectrophotometer.

Results and discussion

In our work, a fourth generation HPAE-OHs4 with surface hydroxyl groups was prepared according to the previous paper [28] with a few modifications. The synthesis route is shown in Scheme 1a. In order to minimize the side reaction between the AB_2 monomer, the choice of effectively available transesterification catalysts which showed the better compromise between chemselectivity and activity has attracted growing attention in chemical reactions. It showed that titanates and zirconates were the most interesting catalysts [29]. Due to above reasons, *p*-methylbenzene sulfonic acid (*p*-TsOH) was replaced by $Ti(OiPr)_4$. The final products of HPAE-OHs4 are soluble in water, ethanol, and *N*, *N*-dimethylformamide (DMF).

HPAE-co-PLGA copolymers can be synthesized through a ring-opening polymerization and polymerization of DL-lactide and glycolide can be affected by at least four different mechanisms categorized as anionic, cationic, coordination, and radical, among which the coordination polymerization is one of the most versatile methods for preparing PLGA and its copolymers and can afford high molecular weights and conversions. In the present polymerization system, metal species are believed to function as a catalyst and the hydroxyl end group of HPAE serves as an initiator.

The active hydrogen atom at one end of the HPAE chains acts as an initiator and induced a selective acyl-oxygen cleavage of DL-lactide and glycolide. The polymerization route is shown in Scheme 1b. The solubility of HPAE-co-PLGA is opposite to HPAE-OHs4, which can be dissolved in acetone, dichloromethane, and tetrahydrofuran (THF). It indicated that PLGA segment was conjugated onto the HPAE-OHs4.

The hydroxyl values of different generation HPAE-OHs were measured and calculated as described in the previous paper [26]. The results of different generation HPAE-OHs are shown in Table 1. It clearly shows that with the increase of generation the hydroxyl values are closer to the theoretical value. It indicates that the structure is apt to regulation.

The different samples, namely, the HPAE-co-PLGA of 6:1 (feed ratio of DL-lactide/glycolide molar ratio), HPAE-co-PLGA of 10:1, and HPAE-co-PLGA of 15:1, respectively, were synthesized.

The molecular weights and polydispersity index of the HPAE-co-PLGA copolymers are shown in Table 2. The amount of lactide introduced to HPAE-OH4 increased with the increase of the molar ratio of DL-lactide/glycolide to HPAE-OH4. As the molar ratios of DL-lactide/glycolide to HPAE-OH4 increased from 6:1 to 15:1, the molecular weights rose from 23 to 76 kDa. This indicates that the higher the concentration of DL-lactide and glycolide, the higher the opportunity of the DL-lactide and glycolide will react with HPAE-OH4 reactive centers.

The hydrophobicity of the copolymer increased in order of HPAE-co-PLGA (6/1), HPAE-co-PLGA (10/1), and HPAE-co-PLGA (15/1) with the increase of the molar ratio of DL-lactide/glycolide in the PLGA segment because DL-lactide unit more hydrophobic than glycolide.

Figure 1a, b shows the FT-IR of the HPAE-OHs4 and HPAE-co-PLGA copolymer. The absorption band of HPAE-co-PLGA at 3,455 cm^{-1} is attributed

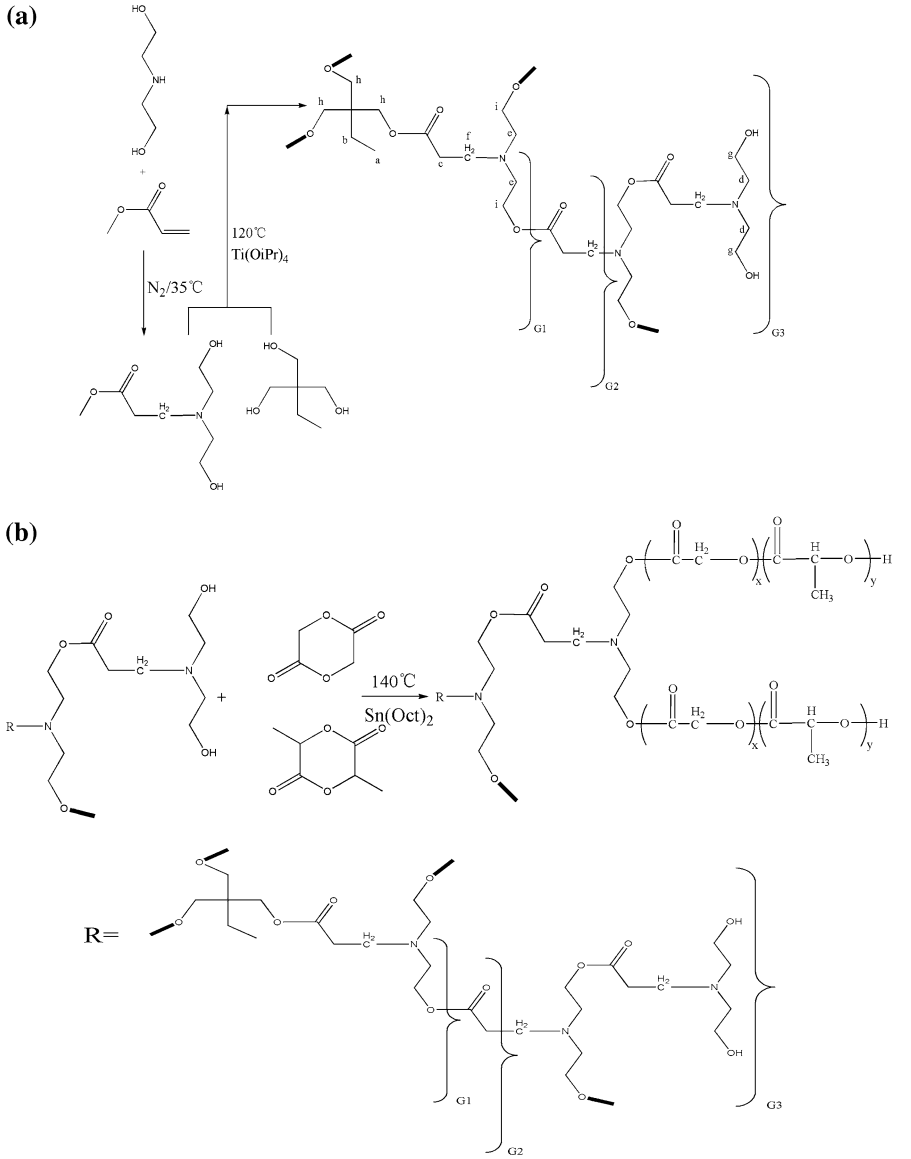

Scheme 1 The synthesis route of HPAE-OHs (**a**) and HPAE-co-PLGA copolymer (**b**)

Table 1 The hydroxyl values of different generation HPAE-OHs

Hydroxyl values of different generation HPAE-OHs	G2	G3	G4
Theoretical value (mgNaOH/g)	306	276	263
Experimental value (mgNaOH/g)	322	250	273

Represent the generation of HPAE-OHs; HPAE-OHs4 (M_w = 7,200 Da)

Table 2 Composition and molecular weight distribution of HPAE-co-PLGA copolymers

Sample	Copolymer	Molecular weight of copolymer		Polydispersity (M_w/M_n)
		M_w (kDa)	M_n (kDa)	
1	HPAE-co-PLGA(6/1)	23	17	1.35
2	HPAE-co-PLGA(10/1)	41	26	1.58
3	HPAE-co-PLGA(15/1)	76	53	1.43

Measured by GPC

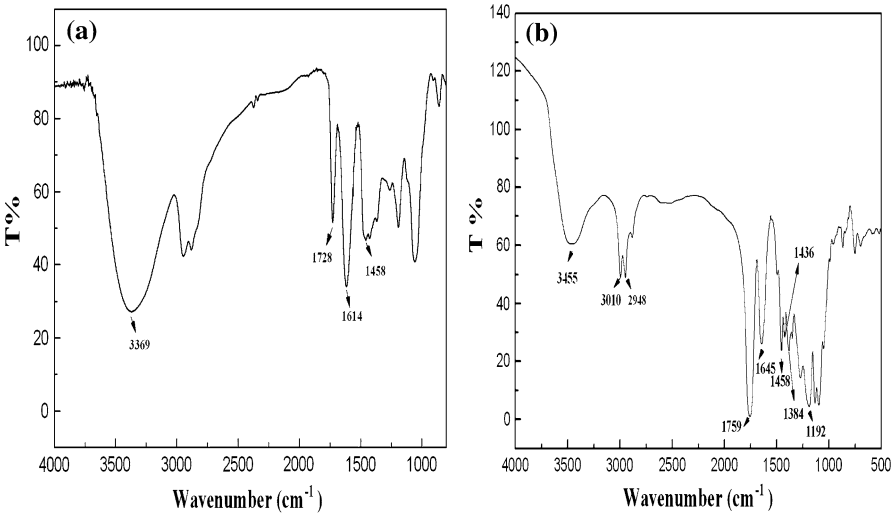

Fig. 1 FT-IR spectra of HPAE-OHs4 (**a**) and HPAE-co-PLGA copolymer (6:1) (**b**)

to terminal hydroxyl groups in the copolymer. The bands at 3,010 and 2,948 cm^{-1} represent C–H stretch of CH_3. A strong band at 1,759 cm^{-1} corresponds to C=O stretch. The CH_2 scissoring and wagging modes at 1,458, 1,436, and 1,384 cm^{-1} are different between the two graphs. For the fourth generation of HPAE-OHs4 (Fig. 1a), the intensity of the three absorption bands is weak and almost equal, while in HPAE-co-PLGA copolymer, the bands located at 1,458 and 1,384 cm^{-1} become much stronger than the other bands. The band at 1,192 cm^{-1} corresponds to the C–O stretching vibration in HPAE-OHs4, while in HPAE-co-PLGA copolymer the absorption intensity becomes stronger than HPAE-OHs4.

The basic chemical structure of HPAE-OHs4 and HPAE-co-PLGA copolymer is also confirmed by ^{1}H-NMR (Fig. 2a, b). Compared with HPAE-OHs4 (Fig. 2a), the ^{1}H-NMR spectra of the HPAE-co-PLGA copolymer (Fig. 2b) shows that the signal at $\sim$4.3 ppm is attributed to the terminal of the methyl proton of the branched polylactide. The signals at $\sim$1.4 and $\sim$1.5 ppm are attributed to the methyl protons of the polylactide moiety located at the terminal groups and the repeat units, respectively. Overlapping doublets at $\sim$1.55 ppm are attributed to the methyl

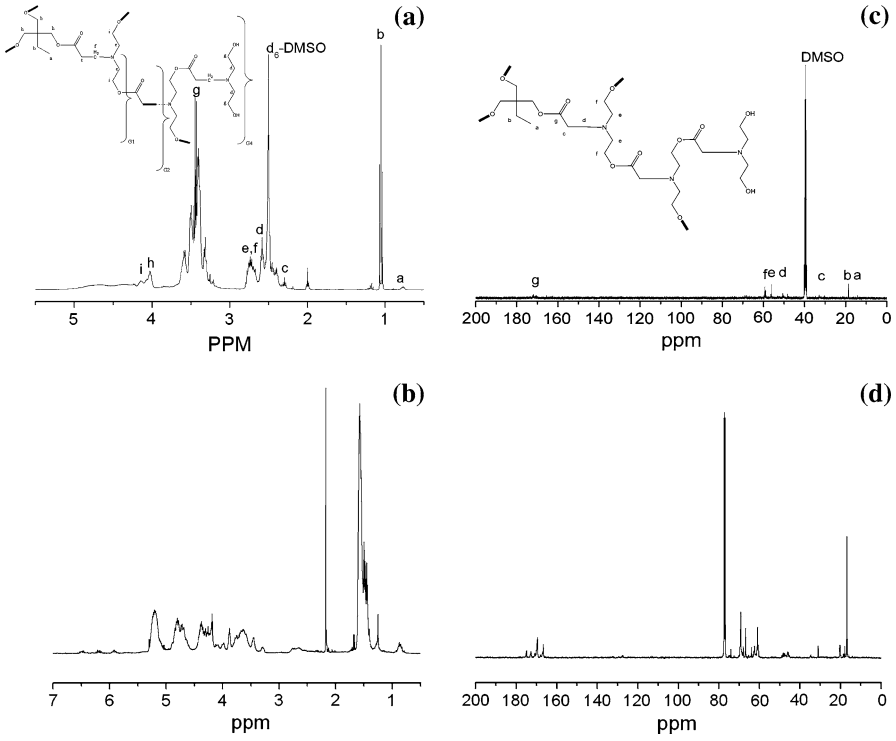

Fig. 2 The exhibited the typical ^{1}H-NMR spectrum of HPAE-OHs4 (**a**), HPAE-co-PLGA copolymer (6:1) (**b**), ^{13}C-NMR spectrum of HPAE-OHs4 (**c**), and HPAE-co-PLGA copolymer (6:1) (**d**)

groups of the D- and L-lactic acid repeat units. The multiplets at ~5.2 and ~4.8 ppm correspond to the lactic acid CH and the glycolic acid CH_2, respectively. The high complexity of the peaks results from different D-lactic, L-lactic, glycolic acid sequences in the polymer backbone (structure of the HPAE-co-PLGA copolymer shown in Scheme 1b).

The basic chemical structure of HPAE-OHs4 and HPAE-co-PLGA copolymer is further confirmed by ^{13}C-NMR (Fig. 2c, d). Compared with HPAE-OHs4 (Fig. 2c), the ^{13}C-NMR spectra of the HPAE-co-PLGA copolymer (Fig. 2d) shows that the peak at ~170 ppm is attributed to the C=O group carbon peak of PLGA moiety. The signals at ~68 and ~70 ppm are assigned to –CH group carbon peak of the PLGA moiety located at the terminal groups and the repeat units, respectively. The signals at ~17 and ~20 ppm are attributed to the $–CH_3$ group carbon peak of the PLGA moiety located at the repeat units and the terminal groups, respectively. All these results evidence that the hyperbranched copolymers contain side chains of polylactide and polyglycolide.

The thermal properties of HPAE-OHs4 and HPAE-co-PLGA copolymers are examined by TGA measurement. Figure 3a shows the TGA thermogram of HPAE-OHs4 and HPAE-co-PLGA copolymers. Compared with HPAE-OHs4, HPAE-co-PLGA copolymers have lower thermal degradation temperature. A fast

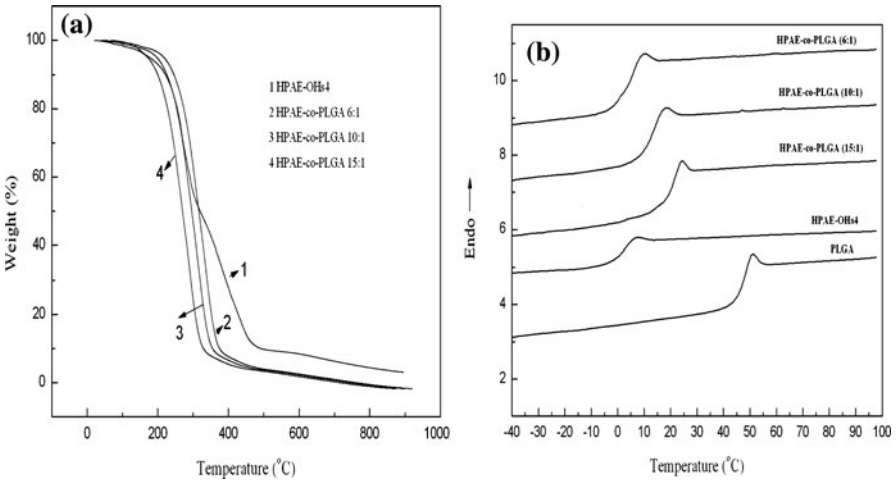

Fig. 3 TGA graphs of HPAE-OHs4, HPAE-co-PLGA copolymers (6:1, 10:1, 15:1) (**a**) and DSC thermo grams of HPAE-OHs4, HPAE-co-PLGA copolymers (6:1, 10:1, 15:1), and PLGA ($M_w = 34$ kDa) (**b**)

process of weight loss appeared in the TGA curves response for the HPAE-co-PLGA copolymers in thermal degradation ranges. The thermo decomposition rate and carbolic survivor increased with the increase of the ratio of PLGA in the copolymers. These results showed that the thermal stability of HPAE-co-PLGA copolymer increases relatively to the original HPAE-OHs4 and the thermal stability of the copolymer decreased with the increase of PLGA segment.

The DSC of HPAE-OHs4, PLGA, and the HPAE-co-PLGA copolymers is measured and the representative DSC traces are shown in Fig. 3b. The T_g of the PLGA segment in the copolymer is 52.1 °C. Only one sidestep presented in all of the samples and it shows no signs of inhomogeneities. The T_gs of the HPAE-co-PLGA copolymers are far lower than that of pure PLGA. It could be explained that HPAE-OHs4 with low T_g was elastic state at room temperature. The decrease in the T_g of PLGA after being grafted on HPAE-OHs4 indicates that the HPAE-OHs4 unit can plasticize the adjacent PLGA chain.

The plots of weight loss versus time are demonstrated on Fig. 4. It indicates that the hydrophilicity–hydrophobicity balance plays an important role in the biodegradation of the HPAE-co-PLGA copolymers and their micelles. Since HPAE unit is hydrophilic, water can diffuse into the HPAE-co-PLGA copolymer matrix, so that the biodegradation takes place simultaneously inside the copolymer film. In addition, the HPAE-co-PLGA copolymer and their micelles with small molecular weight are biodegraded with higher rate than those with high molecular weight. It could be explained that the polymeric chains of small molecular weight have better mobility and are more hydrophilicity, so that it is easier for the water molecules to penetrate into the polymer matrix. The biodegradation behavior could be adjusted through altering hydrophilicity–hydrophobicity balance of the copolymers (micelles) in macromolecular structure, by adjusting copolymer molecular weight,

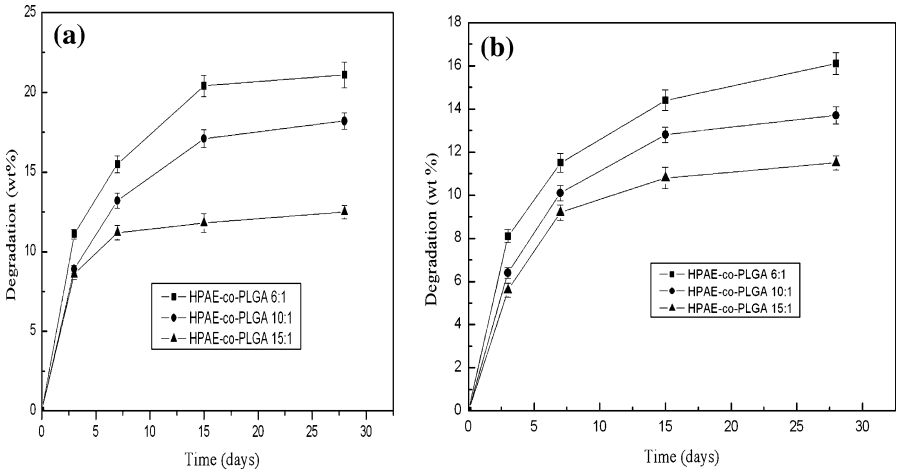

Fig. 4 Weight loss of the HPAE-co-PLGA copolymers (**a**) and HPAE-co-PLGA copolymer micelles (**b**) in PBS (pH 7.4) at 37 °C

crystallinity, and different incubation time as well as adjusting the ratio of DL-lactide/glycolide and DL-lactide/glycolide to HPAE. As a result, the degradation rates of copolymers (micelles) can be changed with a wide range, making it very useful in drug delivery system.

It is well known that amphiphilic copolymers with a suitable hydrophilic/hydrophobic balance can form a micellar structure when exposed to a selective solvent. The HPAE-co-PLGA copolymers, consisting of hydrophilic HPAE and hydrophobic PLGA segments, provide an opportunity to form micelles in water. The micelle behavior of HPAE-co-PLGA copolymer in aqueous media was monitored through fluorometry with the presence of pyrene as a fluorescence probe. In studying the micelles formation of hydrophobically modified copolymer in aqueous solution, pyrene is generally used as a molecular probe, and the variation in the ratio of intensity of first (372 nm) to third (383 nm) vibronic peaks I_{372}/I_{383}, the so-called polarity parameter, is quite sensitive to the polarity of microenvironment where pyrene is located. Figure 5a, b shows the excitation spectra of pyrene in its aqueous solutions with various concentrations and the changes of I_{372}/I_{383} with the concentration. At lower concentrations, I_{372}/I_{383} values remained nearly unchanged. With further increase of concentration, the intensity ratio starts to decrease, implying the onset of micelle from hyperbranched copolymer. The critical micelle concentration (cmc) was determined by the interception of two straight lines. The cmc values of hyperbranched copolymer are listed in Table 3. From the table, we can see that the cmc values of polymeric amphiphilies are lower than the cmc of low molecular weight surfactants [30], indicating the stability of micelles from hyperbranched copolymer at dilute conditions. The increase of hydrophobicity through introduction of a large amount of hydrophobic groups further reduces the cmc values (Table 3).

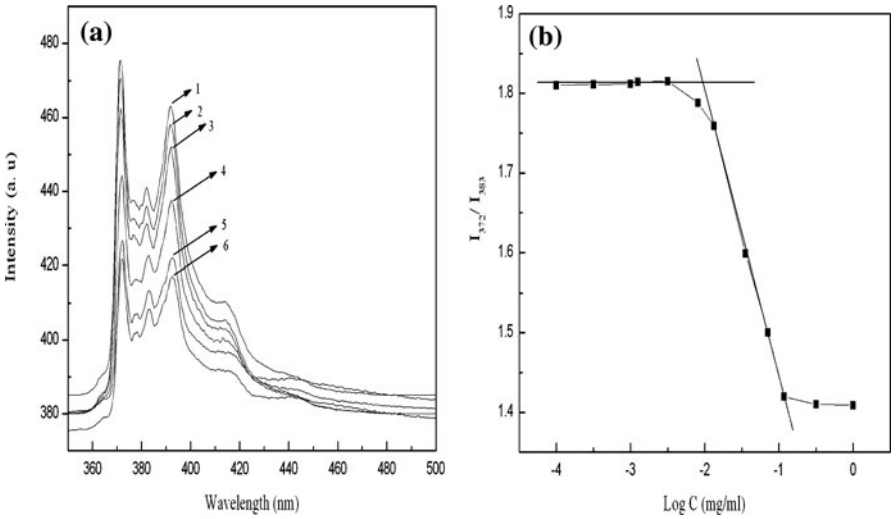

Fig. 5 **a** Fluorescence emission spectra of pyrene in water in the presence of the HPAE-co-PLGA copolymer (10:1) at 20 °C (1:0.5, 2:0.25, 3:0.1, 4:0.01, 5:0.005, 6:0.001 mg/mL). (**b**) Change of the intensity ratio (I_{372}/I_{383}) versus the concentration of the HPAE-co-PLGA copolymer (10:1) at 20 °C

Table 3 Effect of different composition of copolymer on the properties of polymeric micelles and amphotericin B-loaded polymeric micelles

Sample	Copolymer	Mean diameter (nm)	Polydispersity index of mean diameter	cmc × 10^2 (mg/mL)
1	HPAE-co-PLGA(6/1)	114	0.05	5.56
2	HPAE-co-PLGA(10/1)	136	0.08	2.01
3	HPAE-co-PLGA(15/1)	153	0.06	0.99
AmNP6	HPAE-co-PLGA (6/1)	131	0.08	4.39
AmNP10	HPAE-co-PLGA (10/1)	155	0.07	1.73
AmNP15	HPAE-co-PLGA (15/1)	177	0.06	0.85

Amphotericin B content 10% (w/w)

Figure 6a, b shows the ESEM image and the size distribution of amphotericin B-loaded polymeric micelles. As we can see from the figure, the amphotericin B-loaded polymeric micelles are spherical in shape (Fig. 6a) and have a unimodal size distribution (Fig. 6b).

In the clinical administration of the nanoparticle suspension, vessel occlusion due to the particle aggregation may occur. The steric stability of nanoparticles in the biological milieu thus becomes an important aspect to be considered. An improved safety profile of amphiphilic copolymer nanoparticles was observed in comparison with the hydrophobic PLGA nanoparticles, which was attributed to the presence of hydrophilic segment on the particles surface to prevent the coagulation cascade. In the preparation of nanoparticles, the surfactant does not really attend the formation of nanoparticles. It acts as a stabilizer for keeping the particles' stability.

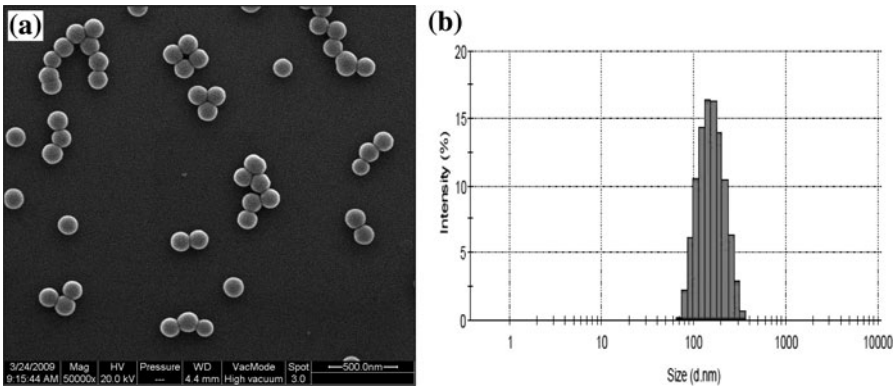

Fig. 6 The ESEM images (**a**) and the size distribution (**b**) of amphotericin B-loaded HPAE-co-PLGA copolymer micelles in water (HPAE-co-PLGA (10:1))

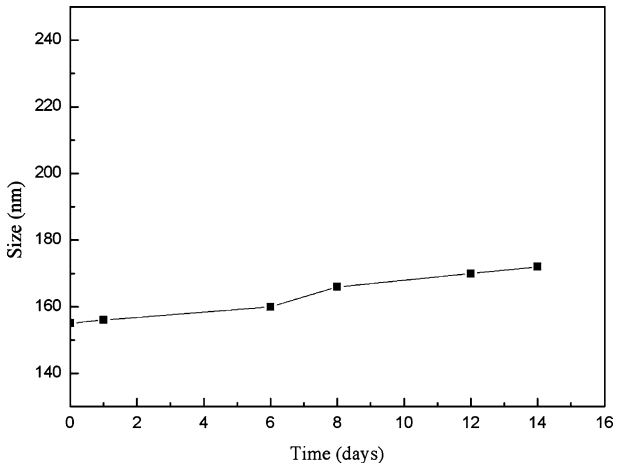

Fig. 7 Steric stability of amphotericin B-loaded HPAE-co-PLGA copolymer micelles (10:1) in PBS

HPAE-co-PLGA copolymer nanoparticles were of an amphiphilic structure: the hydrophobic PLGA segment compromised the pact core while the hydrophilic HPAE-OHS4 segment extended to the outer aqueous environment to form a shell. This structure may have self-stabilization function. In our work, the particles were suspended in PBS and the size was recorded (Fig. 7). Only a small size variation from 155 to 172 nm is observed in 14 days. It demonstrates that HPAE-co-PLGA copolymer nanoparticles possess good steric stability in vitro.

The size and size distribution of polymeric micelles and amphotericin B-loaded polymeric micelles (AmNP6, AmNP 10, and AmNP15) were measured by DLS (Table 3). The size of the plain polymeric micelles was 114–153 nm in water. The DLS data shows that the micelle sizes increased with the increase of molar ratio of DL-lactide/glycolide. These results suggested that the elongation of hydrophobic PLGA side chain facilitates the growth of the hydrophobic core of polymeric

Table 4 Drug loading efficiency, drug entrapment efficiency, and micelle yield of amphotericin B-loaded polymeric micelles

Sample	Copolymer	Entrapment efficiency (%)	Drug loading (%)	Micelle yield (%)
1	HPAE-co-PLGA(6/1)	68.3	7.1	55.2
2	HPAE-co-PLGA(10/1)	73.5	8.5	69.7
3	HPAE-co-PLGA(15/1)	81.7	11.0	85.5

The mass of amphotericin B used was 20% (w/w) in relation to polymer mass

micelles. Table 3 shows that the micelles have a narrow unimodal distribution. The results indicate that the micelle size depends on the ratio of hydrophobic PLGA segment to hydrophilic HPAE segment in the copolymer.

Table 4 summarizes the micelle yield, drug-loading content, and entrapment efficiency of HPAE-co-PLGA copolymeric micelles. The micelle yield and drug-loading content depend mainly on the composition ratio of HPAE to PLGA in copolymers, while drug-loading content in micelles increases from 7.1 to 11.0% with the increase of the ratio of DL-lactide/glycolide to HPAE-OHs4 in copolymers. This result could be explained by the hydrophobic character of amphotericin B. Therefore, the higher the PLGA segment content in copolymer, the easier for the drug to be encapsulated in micelles. HPAE-co-PLGA (15:1) has the highest micelle yield, 85.5%, within all of the samples. A large amount of gelatinous coagulation was found during the acetone evaporation process for preparation of HPAE-co-PLGA (10:1) micelles, which explains the lower micelle yield of the two samples.

Figure 8 showed vitro release profiles of amphotericin B from HPAE-co-PLGA micelles with various DL-lactide/glycolide/HPAE ratios. For all polymeric micelles, amphotericin B release showed both an initial burst release and a release in a sustained manner afterward. During initial burst release, a significant amount of amphotericin B was release within 12 h, 31.56% for HPAE-co-PLGA (6:1) copolymer micelles. After the initial burst, HPAE-co-PLGA release profiles displayed a sustained release. The amount of cumulated HPAE-co-PLGA (6:1) release over 10 days was 77.80% for HPAE-co-PLGA polymeric micelles (amphotericin B content 20%). This sustained release could result from diffusion of amphotericin B into the polymer wall, the drug through polymer wall, and the erosion of the polymer. The release of a drug from the polymer micelles is rather complicated process. It can be affected by many factors such as the polymer degradation, molecular weight, the binding affinity between the polymer and the drug, crystallinity, and so on [31]. In this study, the drug-release rate might be mainly determined by the diffusion of the drug through the polymer matrix. The initial burst might be attributed to the rapid release of drugs in the microchannels probably existing in micelles [32]. Amphotericin B, because of its lipophilic character, was physically entrapped in the hydrophobic core of a micelle. Accordingly, the in vitro release behaviors of a lipophilic compound from the polymeric micelle were largely affected by its inner core with hydrophobic properties [31]. Therefore, as the PLGA content of a copolymer increased, the hydrophobic segments in a copolymer increased, resulting in the increase of the

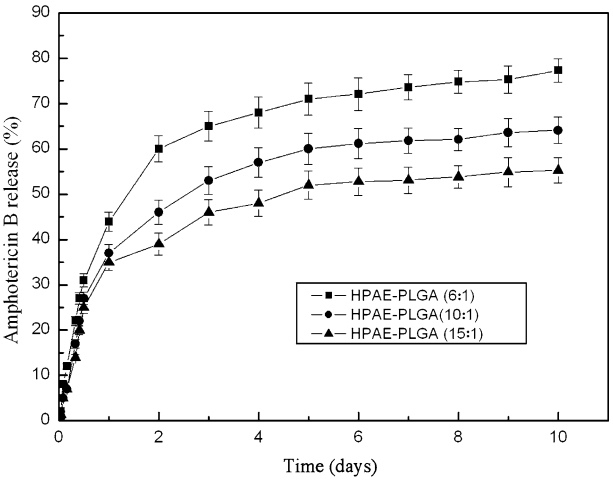

Fig. 8 Release profiles of amphotericin B from HPAE-co-PLGA polymeric micelles

binding affinity between amphotericin B and PLGA. Consequently, in this micelle, the drug-release rate was inversely proportional to the PLGA content of copolymers. Another reason for the fast release rate of HPAE-co-PLGA was their small particle size with relatively large surface area.

Conclusions

Amphiphilic HPAE-co-PLGA copolymers which can form the polymeric micelles were prepared. The hyperbranched copolymers with controlled structure were obtained by adjusting the molar ratio of DL-lactide/glycolide to HPAE unit. The amphotericin B-loaded polymeric micelles were prepared by the phase separation method. The preliminary investigations for the novel micelle have shown that the composition of the copolymer made a great influence on the micelle size, size distribution, and drug release behavior. Control of the micelle size, drug-loading content, and drug release behavior can be achieved by optimizing the ratio of DL-lactide/glycolide to HPAE in the copolymer. The particles suspension exhibited good steric stability in vitro. These results showed that HPAE-co-PLGA polymeric micelles may be a promising new drug delivery system for lipophilic drugs.

Acknowledgment This project was supported by the major program for fundamental research of the Chinese Academy of Sciences, China (No: KJCX2-YW-M02); the State Key Development Program for Basic Research of China (973) (No: 2009CB930200).)

References

1. Hans M, Shimoni K, Danino D, Siegel SJ, Lowman A (2005) Synthesis and characterization of mPEG-PLA prodrug micelles. Biomacromolecules 6:2708–2717
2. Lin R, Ng LS, Wang CH (2005) In vitro study of anticancer drug doxorubicin in PLGA-based microparticles. Biomaterials 26:4476–4485

3. Wang C, Wang C, Hsiue GH (2005) Polymeric micelles with a pH-responsive structure as intracellular drug carriers. J Control Release 108:140–149
4. Agrawal SK, Sanabria-DeLong N, Coburn JM, Tew GN, Bhatia SR (2006) Novel drug release profiles from micellar solutions of PLA–PEO–PLA triblock copolymers. J Control Release 112: 64–71
5. Jiang XZ, Zhang JY, Zhou YM, Xu J, Liu SY (2008) Facile preparation of core-crosslinked micelles from azide-containing thermoresponsive double hydrophilic diblock copolymer via click chemistry. J Polym Sci A Polym Chem 46:860–871
6. Riess G (2003) Micellization of block copolymers. Prog Polym Sci 28:1107–1170
7. Ryu JG, Jeong YI, Kim IS, Lee JH, Nah JW, Kim SH (2000) Clonazepam release from core–shell type nanoparticles of poly(ε-caprolactone)/poly(ethylene glycol)/poly(ε-caprolactone) triblock copolymers. Int J Pharm 200:231–242
8. Lo CL, Huang CK, Lin KM, Hsiue GH (2007) Mixed micelles formed from graft and diblock copolymers for application in intracellular drug delivery. Biomaterials 28:1225–1235
9. Han HD, Shin BC, Choi HS (2006) Doxorubicin-encapsulated thermosensitive liposomes modified with poly (N-isopropylacrylamide-co-acrylamide): drug release behavior and stability in the presence of serum. Eur J Pharm Biopharm 62:110–116
10. Yoo HS, Park TG (2001) Biodegradable polymeric micelles composed of doxorubicin conjugated PLGA–PEG block copolymer. J Control Release 70:63–70
11. Layre A, Couvreur P, Chacun H, Richard J, Passirani C, Requier D, Benoit JP, Gref R (2006) Novel composite core–shell nanoparticles as busulfan carriers. J Control Release 111:271–280
12. Li YY, Zhang XZ, Kim GC, Cheng H, Cheng SX, Zhuo RX (2006) Thermosensitive Y-shaped micelles of poly(oleic acid-Y-N-isopropylacrylamide) for drug delivery. Small 2:917–923
13. Gao C, Yan D (2004) Hyperbranched polymers: from synthesis to applications. Prog Polym Sci 29:183–275
14. Voit B (2000) New developments in hyperbranched polymers. J Polym Sci A Polym Chem 38:2505–2525
15. Tian HY, Deng C, Lin H, Sun JR, Deng MX, Chen XS, Jing XB (2005) Biodegradable cationic PEG-PEI-PBLG hyperbranched block copolymer: synthesis and micelle characterization. Biomaterials 26:4209–4217
16. Rajesh KK, Muthiah G, Munia G, Tanay G, Donald EB, Souvik M, Jayachandran NK (2006) Blood compatibility of novel water soluble hyperbranched polyglycerol-based multivalent cationic polymers and their interaction with DNA. Biomaterials 27:5377–5390
17. Karger-Kocsis J, Fröhlich J, Gryshchuk O, Kautz H, Frey H, Mülhaupt R (2004) Synthesis of reactive hyperbranched and star-like polyethers and their use for toughening of vinylester-urethane hybrid resins. Polymer 45:1185–1195
18. Gao C, Xu Y, Yan D, Chen W (2003) Water-soluble degradable hyperbranched polyesters: novel candidates for drug delivery? Biomacromolecules 4:704–712
19. Kolhe P, Misra E, Kannan RM, Kannan S, Lieh-Lai M (2003) Drug complexation, in vitro release and cellular entry of dendrimers and hyperbranched polymers. Int J Pharm 259:143–160
20. Kim HJ, Kwon MS, Choi JS, Kim BH, Yoon JK, Kim K, Park JS (2007) Synthesis and characterization of poly (amino ester) for slow biodegradable gene delivery vector. Bioorg Med Chem 15:1708–1715
21. Jeong B, Bae YH, Kim SW (2000) Drug release from biodegradable injectable thermosensitive hydrogel of PEG-PLGA-PEG triblock copolymers. J Control Release 63:155–163
22. Blanco MD, Alonso MJ (1997) Development and characterization of protein-loaded poly (lactide-co-glycolide) nanospheres. Eur J Pharm Biopharm 43:287–294
23. Yang R, Yang SG, Shim WS, Cui F, Cheng G, Kim IW, Kim DD, Chung SJ, Shim CK (2009) Lung-specific delivery of paclitaxel by chitosan-modified PLGA nanoparticles via transient formation of microaggregates. J Pharm Sci 98:970–984
24. Thomas PA (1994) Mycotic keratitis-an underestimated mycosis. J Med Vet Mycol 32:235–256
25. Essman TF, Flynn HW Jr, Smiddy WE, Brod RD, Murray TG, Davis JL, Rubsamen PE (1997) Treatment outcomes in a 10-year study of endogenous fungal endophthalmitis. Ophthalmic Surg Lasers 28:185–194
26. Zhu BK, Wei XZ, Xiao L, Xu YY, Geckeler KE (2006) Preparation and properties of hyperbranched poly (amine-ester) films using acetal cross-linking units. Polym Int 55:63–70
27. Dong YC, Feng SS (2004) Methoxy poly(ethylene glycol)-poly(lactide) (MPEG-PLA) nanoparticles for controlled delivery of anticancer drugs. Biomaterials 25:2843–2849

28. Lu Y, Lin D, Wei HY, Shi WF (2001) Synthesis and characterization of hyperbranched poly(amine-ester). Acta Polymer Sin 4:411–414
29. Karayannidis GP, Roupakias CP, Bikiaris DN, Achilias DS (2003) Study of various catalysts in the synthesis of poly (propylene terephthalate) and mathematical modeling of the esterification reaction. Polymer 44:931–942
30. Zhang LM (2001) Cellulosic associative thickeners. Carbohydr Polym 45:1–10
31. Shin IG, Kim SY, Lee YM, Cho CS, Sung YK (1998) Methoxy poly(ethylene glycol)/ε-caprolactone amphiphilic block copolymeric micelle containing indomethacin. I. Preparation and characterization. J Control Release 51:1–11
32. Niwa T, Takeuchi H, Hino T, Kunou N, Kawashima Y (1993) Preparations of biodegradable nanospheres of water-soluble and insoluble drugs with D, L-lactide/glycolide copolymer by a novel spontaneous emulsification solvent diffusion method, and the drug release behavior. J Control Release 25:89–98